Hindawi
Advances in Civil Engineering
Volume 2024, Article ID 6637911, 17 pages
https://doi.org/10.1155/2024/6637911

Research Article

Effects of Cement Treatment on Water Retention Behavior and Collapse Potential of Gypseous Soils: Experimental Investigation and Prediction Models

Hussein Q. Abdulameer AlNaddaf,[1] **Saeed Kouzegaran**,[2] **Mohammed Y. Fattah**,[3] **and Ali Akhtarpour**[1]

[1]*Department of Civil Engineering, Faculty of Engineering, Ferdowsi University of Mashhad, Mashhad, Iran*
[2]*Faculty of Technology and Engineering, University of Mazandaran, Babolsar, Iran*
[3]*Civil Engineering Department, University of Technology, Baghdad, Iraq*

Correspondence should be addressed to Ali Akhtarpour; akhtarpour@um.ac.ir

Received 1 September 2023; Revised 3 November 2023; Accepted 11 December 2023; Published 16 January 2024

Academic Editor: Elisabete Teixeira

Gypseous soil poses a significant challenge in geotechnical engineering due to its susceptibility to collapse under saturation. This type of soil covers approximately 33% of regions in Iraq, primarily in unsaturated conditions. This study focuses on two types of gypseous soils: one with moderate gypsum content from Karbala city (G1) and the other with high-gypsum content from Tikrit city (G2), to investigate the effects of cement treatment on their water retention behavior and potential for reducing collapse. Different percentages of cement were mixed with both soils to determine the optimum soil–cement mixture for reducing collapse potential (CP) through single oedometer tests. The water retention characteristics and water retention behavior of samples with varying gypsum content and different levels of cement treatment were examined and compared using a controlled-suction oedometer. The soil–water retention curve (SWRC) of these natural and treated gypseous soils was also investigated and compared in both wetting and drying paths. Additionally, multiple pedotransfer functions (PTFs) were assessed to identify or adapt prediction equation(s) for the SWRC of gypseous soil both with and without cement treatment with acceptable accuracy. The results show that adding cement can decrease the CP of gypseous soils; it also affects their SWRC significantly. By making some simple modifications, the PTFs demonstrate acceptable estimations for the water retention curve of both natural and cement-treated gypseous soils.

1. Introduction

Gypseous soils refer to soils containing enough gypsum content to change or affect their engineering properties and are widespread in many regions worldwide (e.g., it covers approximately 33% of Iraq's areas) mainly in unsaturated conditions. They are usually characterized as collapsible and problematic soils. The primary geotechnical issue with these soils is their susceptibility to significant shear strength reduction, volume reduction, and progressive settlements when exposed to water flow caused by rainfall, irrigation, broken water lines, ground water rise, and so on [1–6].

Recent studies have shown that the chemical stabilization can enhance the characteristics of collapsible soil [5, 7–9]. Hayal et al. [3] investigated the effects of nanosilica on the reduction of collapse potential (CP) in gypseous soil and found that even a small amount of nanosilica could reduce CP by up to 91%. However, the addition of further stabilizer can increase the CP. In another study, Ibrahim [4] examined the potential for enhancing gypseous soil by mixing it with cement at various concentrations. The results showed that the reduction in collapsibility was about 87%–92% for a 12% mixed cement to soil ratio.

The previous investigations on gypseous soils have primarily concentrated on their response in either dry or saturated states. Nevertheless, in natural environments, soils undergo variations in water content, and soil layers near the surface remain in unsaturated state during certain periods throughout the year. Recognizing the distinctions in mechanical behavior

between saturated and unsaturated soils, the differentiation between these states is considered crucial [10].

Matric suction (the difference between pore air and water pressures (ua−uw)), which relates to the soil–water content, is a critical factor in the mechanical behavior of unsaturated soils. The soil–water retention curve (SWRC), defines the relationship between soil suction and its water content [10–13]. The creation SWRCs enable the geotechnical experts to characterize the suction behavior of unsaturated soil and effectively address the diverse geotechnical engineering challenges related to slope stability, foundation bearing capacity, seepage, permeability, and shear strength properties of unsaturated soil [14–17]. While significant advances have been made in the field of unsaturated soil mechanics in recent years, there is still a notable gap in our understanding of the unsaturated water retention behavior of cementitious stabilized soil, especially in gypseous soil. Despite its common use in various ground improvement projects, this soil type has not been thoroughly studied in terms of its suction characteristics. In this regard, Emery et al. [18] studied the effects of stabilization with cement and lime on the SWRC of clayey soil. Their comprehensive laboratory testing and data analysis revealed that while stabilization with lime reduced the air-entry potential, stabilization with cement enhanced it.

Various experimental methods are available for measuring soil suction and the corresponding SWRC. These methods include both direct methods, such as pressure plates, and tensiometers, as well as indirect techniques, such as contact/noncontact filter paper, and heat dissipation sensors [19, 20] However, the utilization of these methods is frequently associated with time-consuming and costly procedures. Consequently, numerous research has focused on the development of pedotransfer functions (PTFs) aiming to estimate SWRC parameters. These PTFs utilize basic soil characteristics such as soil gradation, Atterberg limits to estimate SWRC parameter [21–37].

1.1. Objectives and Outline of This Study. As mentioned before, the behavior of gypseous soils in unsaturated conditions and their water retention potential under different matric suctions remain largely unknown. To address this critical knowledge gap, this research aims to deepen our understanding of gypseous soils with different gypsum contents and their water retention potential which serves as a fundamental factor which control the unsaturated soil behavior. It also seeks to advance predictive capabilities through the development or refinement of PTFs for estimating the SWCC of gypseous soils. Moreover, this study evaluates their susceptibility to collapse, and the potential of cement stabilization as a mitigation technique and assesses the impact of cement stabilization on the soil–water retention potential.

To these aims, the study employs single oedometer tests (SOTs) to determine the optimum soil–cement mixture for mitigating the CP of gypseous soils. Additionally, it explores and compare the water retention behavior of pure and cement-treated gypseous soils, utilizing a controlled-suction oedometer apparatus. To facilitate predictive modeling, an evaluation of various existing PTFs is conducted to identify or refine a prediction method that can accurately estimate the water retention curve of gypsum soil.

Table 1: Physical properties of soils.

Physical properties	G1	G2
Gypsum content (%)	18	66
Specific gravity (Gs)	2.38	2.54
Initial water content (%)	6.7	7.1
Field dry density (g/cm³)	1.61	1.638
Classification	SP	SP

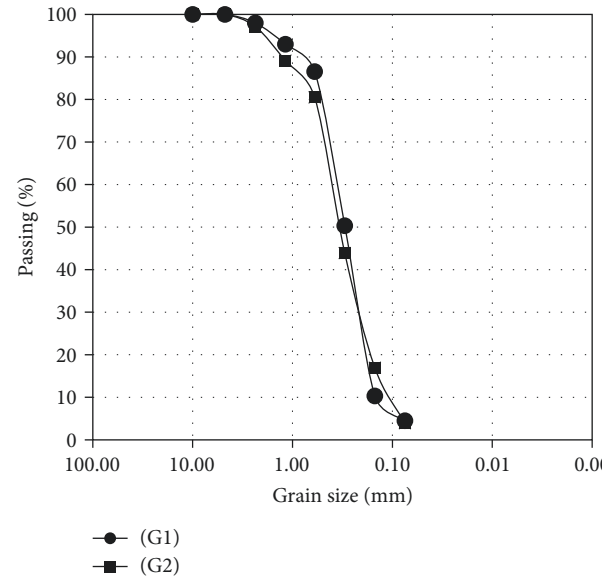

Figure 1: Grain size distributing of G1 and G2 soils.

2. Laboratory Study

2.1. Soil and Material

2.1.1. Gypseous Soil. The soils used in this study are collapsible sandy gypseous soils. Soil samples were collected from two different locations: Karbala holy city (G1) with 18% gypsum content and Tikrit university site (west of Iraq) (G2) with 66% gypsum content. All samples are representing disturbed soils. The sand replacement method was used to calculate the soil's field dry density, and the values were 1.61 gm/cm^3 for G1 and 1.638 gm/cm^3 for G2. The physical parameters of the soil are presented in Table 1, and the grain size distribution for the G1 and G2 samples is shown in Figure 1. To ensure comparability, both soils were prepared with similar gradations using sieve analysis in accordance with the American Society for Testing and Materials' requirements, both soils are classified as poorly graded sand (SP) based on the unified soil classification system according to ASTM D-422 [38].

2.1.2. Portland Cement (Sulfate Resistance). The Portland cement utilized in this work was locally manufactured in Iraq, and considering the gypsum content of soils, sulfate

Table 2: Chemical components of cement.

Chemical components	Value
Sulfate content SO_3 (%)	2.29
Tricalcium aluminates, C_3A (%)	3.27
Magnesium oxide, MgO (%)	3.62
Chloride content (%)	0.02
Finesse	330

resistance cement was used. Its chemical components are listed in Table 2.

2.2. Samples Preparation and Testing Details

2.2.1. Standard Proctor Test. The Proctor tests were conducted according to ASTM D698-00a [39] for the pure gypseous soils G1 and G2, as well as gypseous soils treated with cement "G1 + 1%, 3%, and 5%" and "G2 + 1%, 3%, and 5%", to obtain the optimum moisture content (OMC) and maximum dry density.

2.2.2. Single Oedometer Test (SOT). SOTs were performed according to ASTM D5333 [40] to investigate the collapsibility of gypseous soils under saturated conditions. To obtain the optimum soil cement percentage for reduction of CP, the soil was treated with different cement contents (i.e., 1%, 3%, and 5%) for these tests, and the CP results were compared. The soil utilized passed sieve # 4 (4.75 mm), and the size of the samples was 50 mm in diameter and 20 mm in height. They were prepared at a density of 90% of the maximum dry density with OMC obtained from standard compaction test for pure soils (G1 and G2). The pure soils were tested immediately after preparing the samples, while the treated soil samples were kept in desiccator for 7 days for curing.

During the tests, the soil samples underwent incremental loading at initial conditions until reaching a vertical stress of 200 kPa with a load increment ratio of 1. Subsequently, the samples were soaked in water for 24 hr, and the additional settlement at 200 kPa resulting from the soaking process was measured. The testing continued with further loading and unloading stages.

The CP was calculated using the following equation:

$$Cp = \frac{\Delta He}{Ho} = \frac{\Delta e}{1 + eo} \times 100\ . \quad (1)$$

Tables 3 and 4 present two criteria usually used to classify the gypseous soils.

2.2.3. Controlled-Suction Oedometer. In the current study, a controlled-suction oedometer apparatus was used to obtain the SWRC for pure gypseous soils (G1 and G2) and the improved gypseous soils with optimum cement contents (G1 + optimum cement content) and (G2 + optimum cement content). The schematic shape and the control panels of this device are illustrated in Figures 2 and 3, respectively. The unsaturated equipment was adjusted and calibrated as defined by Fredlund and Rahardjo [12, 13]. Soil was dried in an oven with 45°C and then samples were prepared with 90% of maximum density and OMC, which were obtained from the standard compaction test. As mentioned before, the pure samples were tested immediately after preparing while the samples treated with cement were left for 7 days for curing. The tests were conducted in main wetting path followed by a drying path with volume changes measured throughout. The size of the sample in the oedometer ring test was 5.03 cm in diameter and 1.96 cm in height.

Table 3: The criteria proposed by Jennings and Knight [41] for classification of collapsible soil.

CP (%)	Severity of problem
0–1	No problem
1–5	Moderate trouble
5–10	Trouble
10–20	Severe trouble
20	Very severe trouble

Table 4: Classification of gypseous soil based on collapse index, Ie% (D5333-2003).

Degree of specimen collapse	Collapse index, Ie (%)
None	0
Slight	0.1–2.0
Moderate	2.1–6.0
Moderately Severe	6.1–10.0
Severe	>10

The air and water pressure were set using the data logger, and the change in water volume was measured using the graduated tube. To start the wetting path, an initial 100-kPa suction was applied followed by a step-by-step reduction in matric suction to zero suction. For the following drying path, step-by-step matric suction increment was applied until 100-kPa suction. In each step, the suction was applied until equilibrium was reached, which was determined by monitoring the water level in the graduated tube until no water entered or exited the sample. The water volume change and applied suction were recorded at each step to draw the SWRC.

3. Test Results and Discussion

3.1. Standard Proctor Test. Table 5 presents the results of adding cement to G1 and G2. The effect of different percentages of cement (1%, 3%, and 5%) on the test results was observed through an increase in density and a decrease in OMC of both soils (1 and 2), as shown in Figures 4 and 5.

3.2. Single Oedometer Test. Figures 6 and 7 illustrate the result of the single oedometer test conducted on G1 and G2 soils, both before and after treatment with cement. The summarized results can be found in Table 6. It can be observed that after adding 3% of cement, the coefficient of collapse decreased from 3.97 to 1.05 for G1, indicating a 72% change in CP. This change represents a transition in the degree of specimen collapse from a moderate level to a slight level, based on the collapse index classification criteria (Ie%-D5333-2003). Similarly, for G2, the coefficient of collapse decreased from 7.04 to 1.28 after adding 5% of cement, resulting in an 82% change in CP. This improvement shifted the CP from troublesome to slight.

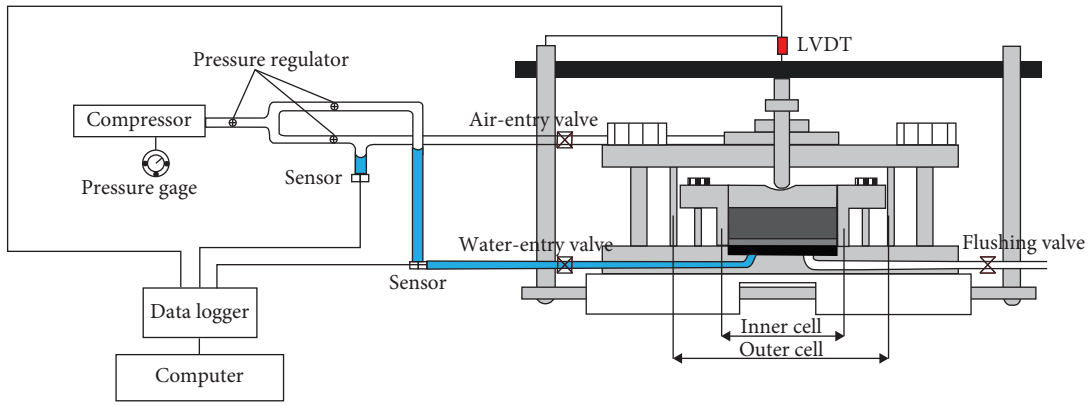

Figure 2: Schematic shape for oedometer device.

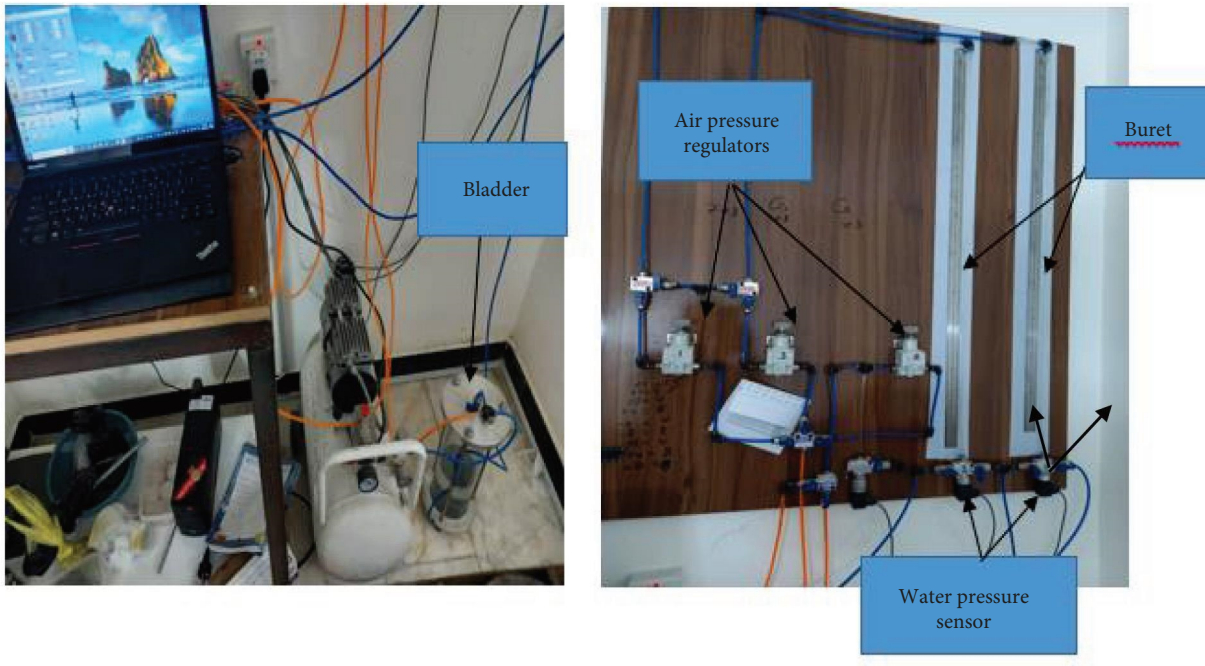

Figure 3: The control boards.

Table 5: Maximum dry density (max. γdry) and optimum moisture content (OMC) of soils.

Physical properties	OMC (%)	(Max. γdry) (g/cm^3)	Physical properties	OMC (%)	(Max. γdry) (g/cm^3)
Pure G1	14.9	1.789	Pure G2	15.5	1.82
G1 + 1% cement	14.5	1.794	G2 + 1% cement	15.0	1.835
G1 + 3% cement	13.5	1.825	G2 + 3% cement	13.7	1.84
G1 + 5% cement	11.3	1.833	G2 + 5% cement	13.0	1.854

In fact, when the gypseous soil samples were fully submerged, the bonds between particles, as well as the gypsum crystals present in these soils, dissolved and brock apart in water; this process weakened the shear strength between the soil grains and led to collapses. However, the treatment of soils by adding cement introduced a different kind of binding that could resist the effects of water. As a result, the CP was reduced when the cement-treated samples were submerged.

3.3. The Soil–Water Retention Curves. In this study, the SWRC of untreated and cement-treated G1 (moderate gypsum content) and G2 (high-gypsum content) soils was investigated in wetting and drying paths using a suction-controlled oedometer device. The differences in SWRC between wetting and drying paths and the observed hysteresis of SWRC is primarily attributed to the ink-bottle effect which is a result of differences in pore-size distribution. Additionally, the generation of trapped air in closed

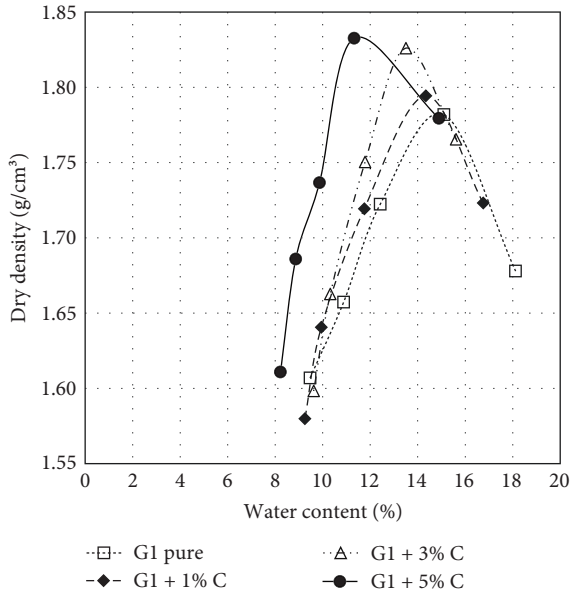

Fugure 4: Compaction test of G1 soil.

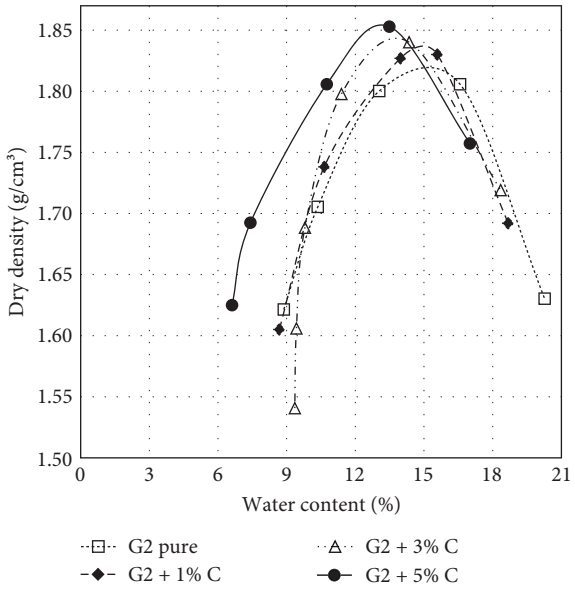

Figure 5: Results of compaction test of G2 soil.

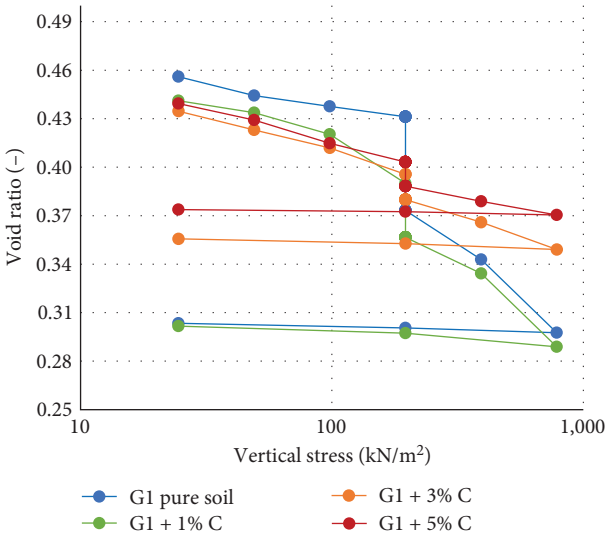

Figure 6: Single oedometer test of pure and treated G1 soil.

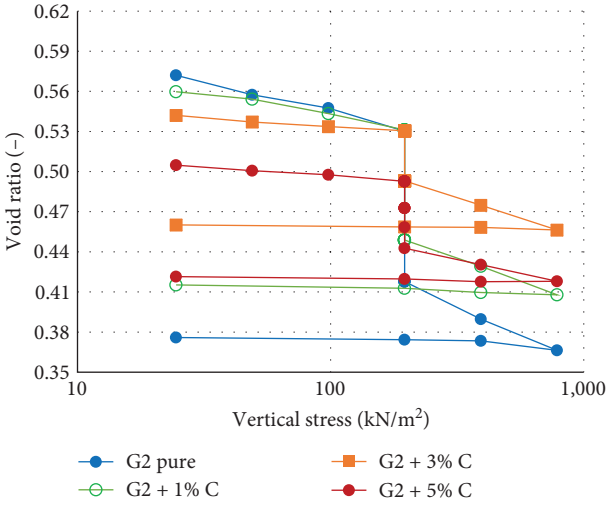

Figure 7: Single oedometer test of pure and treated G2 soil.

pores during the wetting process also plays significant roles in these differences [42].

Figure 8 illustrates the SWRC for G1 and G2 soils before and after cement treatment, separately for the wetting (Figure 8(a)) and drying (Figure 8(b)) paths. The curves clearly show the influence of cement treatment on both soils and paths. It can be observed that the SWRC curve for treated soil lies mostly above that of untreated soil for both G1 and G2 and for both drying and wetting paths. This can be attributed to the increase in the pore-size distribution index due to cement stabilization. The finer soil matrix in the treated samples exhibits a greater capacity to attract and retain water, leading to a higher position of the SWRC curve.

Furthermore, it is noticeable that the effect of cement treatment on the wetting paths is more pronounced than on the drying paths. In other words, the differences between G2 and G2 + 5% in the wetting path are greater than in the drying path, and the same applies to G1. This can be attributed to the solubility of gypseous soil in water. The changes (collapses) in the gypseous soil structure caused by water absorption during the wetting path result in more significant differences between the SWRC of treated and untreated samples compared to the drying path.

To compare untreated and treated samples of G1 and G2 soils separately, their SWRC are shown in Figures 9(a) and 9(b), respectively, for drying and wetting paths. It can be observed that the differences between the wetting and drying curves are more significant in pure samples (G1 and G2) than in the treated soils. This is attributed to the collapsibility potential of untreated gypseous samples during the wetting path. In these untreated samples, the increasing water content during the wetting path gradually dissolves and breaks

Table 6: Changes in degree of specimen collapse due to cement treatment (considering ASTM D5333-2003 criteria).

	CP (%)	Degree of specimen collapse	CP (%)	Changes in CP	Degree of specimen collapse	CP (%)	Changes in CP	Degree of specimen collapse	CP (%)	Changes in CP	Degree of specimen collapse
Cement (%)		Pure samples		1%			3%			5%	
G1	3.79	Moderate	2.25	40%	Moderate	1.05	72.3%	Slight	1.02	73%	Slight
G2	7.04	Trouble	5.19	26.2%	Trouble	2.29	67.4%	Moderate	1.28	81.8%	Slight

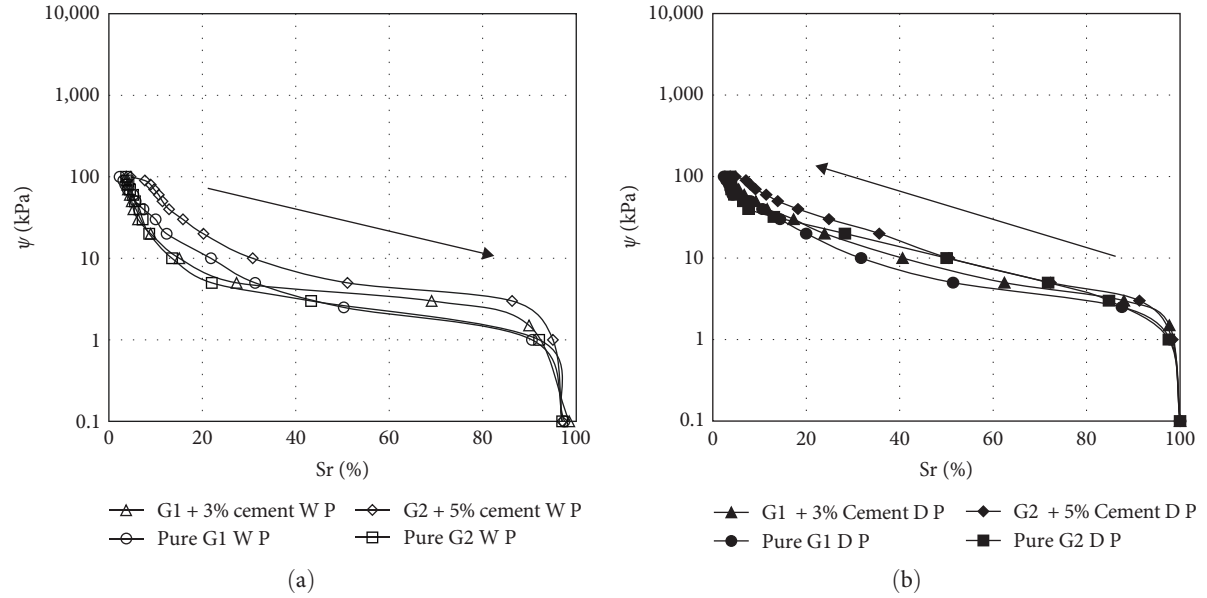

Figure 8: SWRC for pure and treated G1 and G2 soils: (a) wetting paths and (b) drying paths.

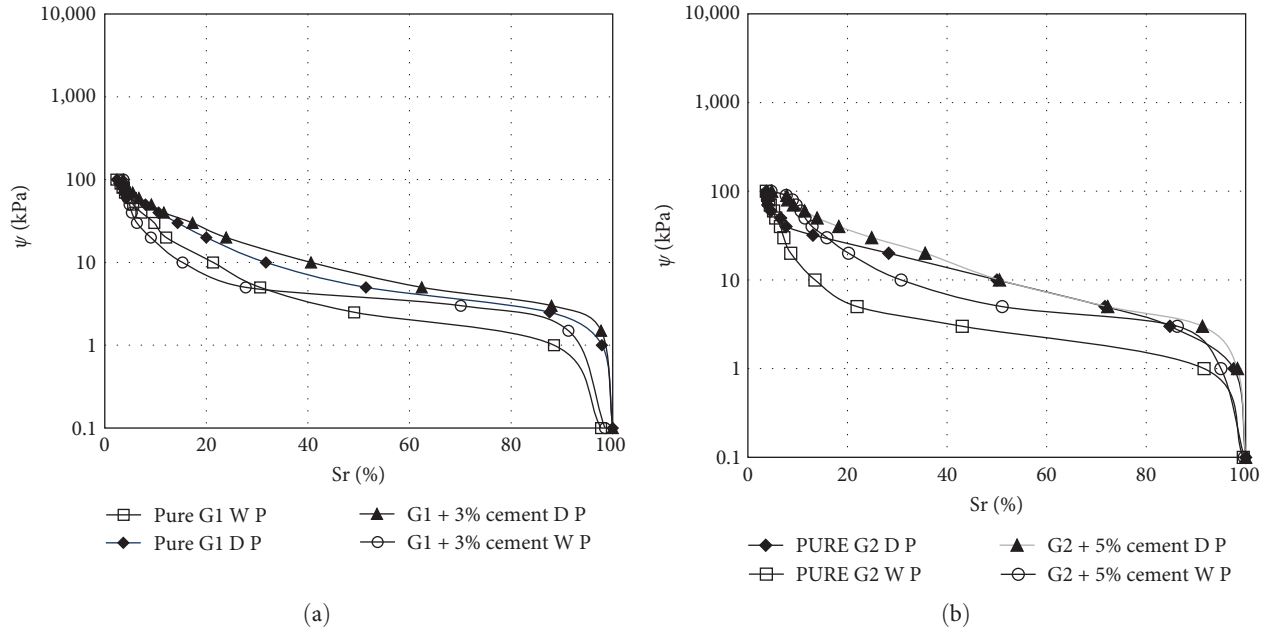

Figure 9: SWRC—wetting and drying paths for pure and treated soil: (a) G1 and (b) G2 soils.

apart the existing gypsum crystals and gypseous bonds between the soil particles. Conversely, in cement-treated samples, the cement bindings can resist the effects of water and remain unchanged during the wetting path. As a result, the wetting path of untreated gypsum soil samples exhibits more significant changes compared to the cement-treated samples.

The effectiveness of cement improvement was also observed in the increase of the air-entry value (AEV) for both the drying and wetting paths of G1 (moderate gypsum content) and G2 (high-gypsum content) soils. Table 7 presents the differences in AEV between the treated and untreated samples.

Table 7: Changing in air-entry values.

Soil type	AEV wetting path (kPa)	AEV drying path (kPa)
G1	1.3	2.6
G1 + 3% cement	2.3	3
G2	1.6	2.1
G2 + 5% cement	3.5	3.9

It can be observed that the stabilization with cement resulted in a slight increase in the AEV for both the drying and wetting paths of G1 and G2 soils. This increase can be attributed to the interaction between the cement and soil

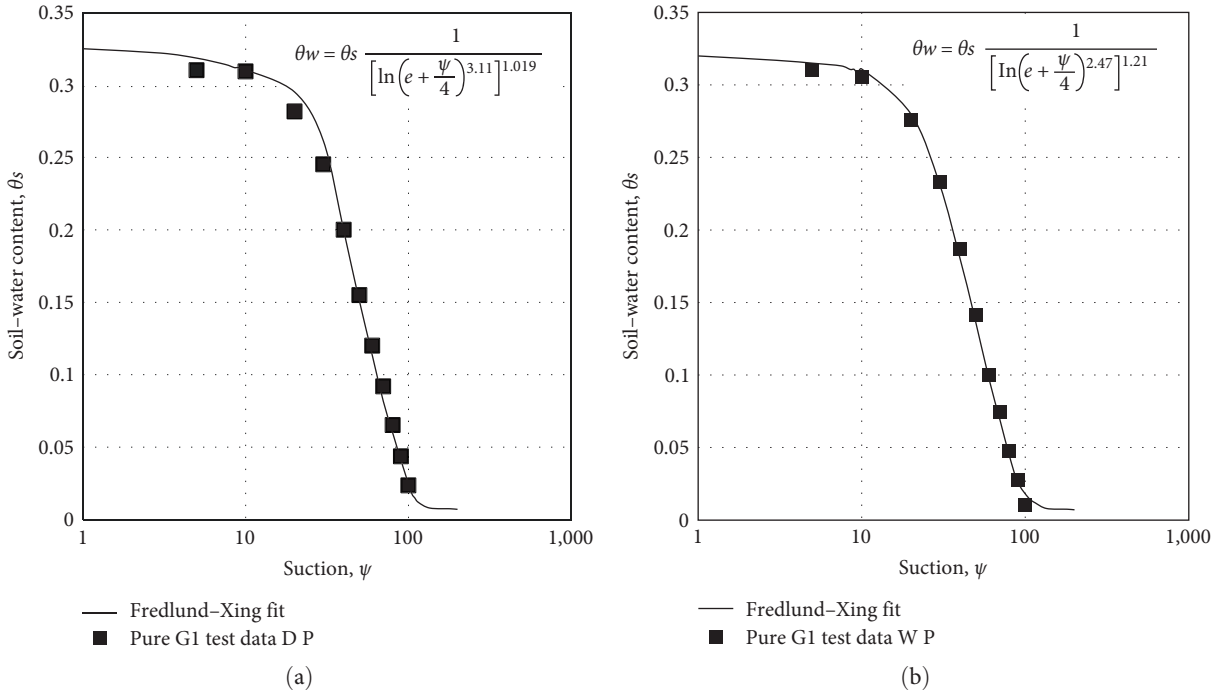

FIGURE 10: Best fitted SWRC for pure G1 and its equation: (a) drying path and (b) pure G1 wetting path.

particles, which enhances the bonding and fills the voids. Consequently, there is an increase in the pore-size distribution index. This indicates that the soil voids are expected to drain water at a slower rate compared to the untreated soil.

It is noteworthy to mention that all the above-mentioned results were more highlighted for G2 soil. This is attributed to its higher gypsum content and resulted CP.

3.4. Fitting Curves. Due to the time-consuming and extensive testing involved in obtaining multiple points on the water retention curve for a specific soil, researchers have developed equations to derive a continuous mathematical representation of the soil–water characteristic curve (SWCC) from a limited number of data points.

3.4.1. Fredlund and Xing Fitting Equation. In the present study, the equations were proposed by Fredlund and Xing [43]. Equation 2 was employed to fit the experimental points obtained through controlled-suction oedometer tests:

$$\Theta = \Theta s \left[\frac{1}{\ln\left[e + \left(\frac{\Psi}{a}\right)^n\right]^m} \right], \quad (2)$$

where

$a = \psi_i$

$m = 3.67 \ln + \left(\frac{\Theta_s}{\Theta_i}\right)$

$n = \frac{1.31^{m+1}}{m^{\Theta s}} 3.72 s\psi_i$

$s = \frac{\Theta_i}{\psi_p - \psi_i}$

Where:

a: is a related parameter that fits with AEV of the soil measure in (kPa). The point $(a, \theta(a))$ can be used to approximate the inflection point in the SWRC curve.

(ψ_i, θ_i): inflection point on the SWRC plot;

θ_s: is the θ when the suction is zero;

n and m: are also fit the parameters; n: is related to the slope of the SWCC, while m is related to the residual water content of the soil;

s: is the slope of tangent line (at the inflection point; i.e., (ψ_i, θ_i);

ψ_p: is the intercept of the tangent line and the matric suction axis in (kPa).

Figures 10–13 depict the fitting curves of untreated and cement-treated samples for both gypseous soils based on this equation. The results demonstrate that the water retention behaviors of both untreated and cement-treated gypseous soils were modeled accurately by Fredlund and Xing [43] equation.

3.4.2. Feng and Fredlund Fitting Model and the Simple Scaling Method. In this study, the Feng and Fredlund [44] SWRC-fitting equation was also evaluated to fit the experimental points obtained through controlled-suction oedometer tests. This method, along with the related scaling method for calculating the main drying and wetting curves from fitted initial drying curve was suggested and used in some previous studies, such as Pham et al. [45] and Johari and Hooshmand Nejad [46].

Following the procedure described by Pham et al. [45] and Johari and Hooshmand Nejad [46], the experimental results of the initial drying paths for pure G1 and G2 soils were fitted and then the main drying and wetting curves were

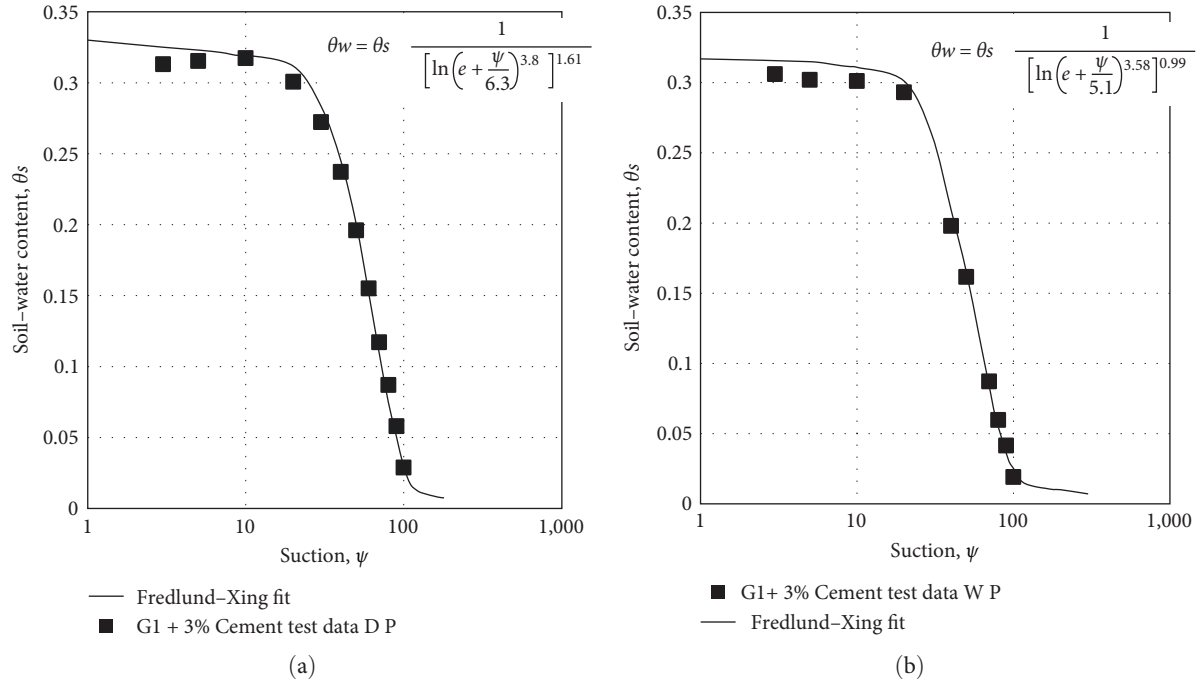

Figure 11: The best fitted SWRC for treated G1 and its equation: (a) drying path and (b) wetting path.

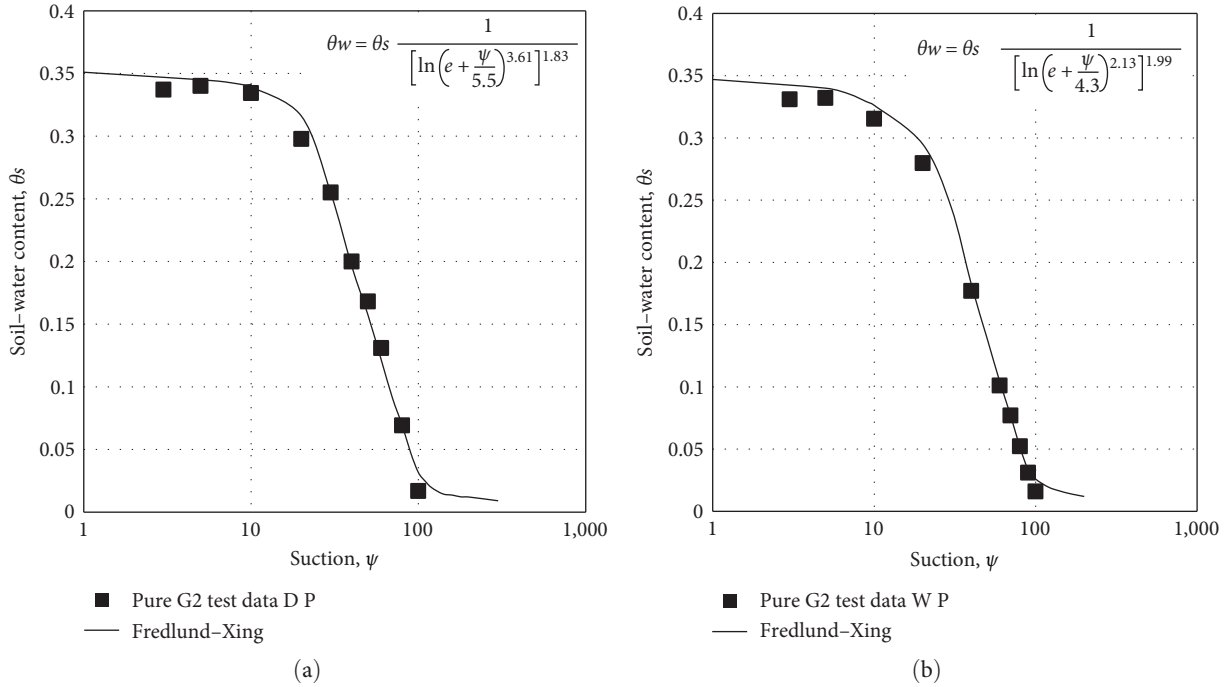

Figure 12: The best fitted SWRC for pure G2 and its equation: (a) drying path and (b) wetting path.

calculated. Table 8 displays the chosen parameters for the fitting curves of Pure G1 and G2. D_{sL} and R_{sL} were set to 2.0 and 0.2, respectively, based on the recommendations from Pham et al. [45] and Johari and Hooshmand Nejad [46] for sandy soils. The obtained results are illustrated in Figures 14(a) and 14(b), where the experimental data points are also included for comparison.

While the initial fitting curve demonstrated acceptable accuracy, it is apparent that the calculated main wetting curve did not align with the experimental results. Notably, the calculated wetting curve is intersecting with both the initial and main wetting curves, which is unacceptable. This variance could be attributed to the fact that in gypseous samples, the increasing water content during the wetting path gradually

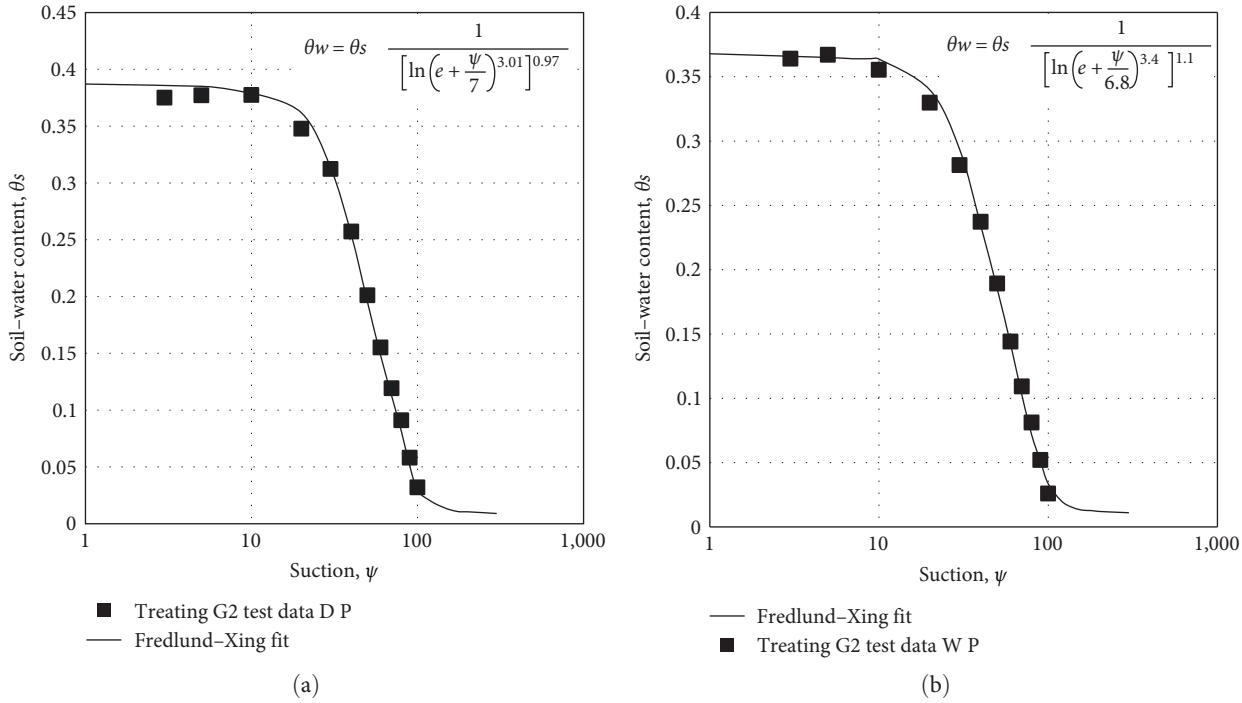

Figure 13: Best fitted SWRC for treated G2 and its equation: (a) drying path and (b) treated G2 wetting path.

Table 8: Chosen values for the fitting curves parameters for pure G1 and G2 and the calculated results.

	Pure G1	Pure G2
Chosen ratio of slopes in semilogarithmic coordinate system, R_{sL}	2.0 (1.2*)	2.0 (1.3*)
Chosen distance in semilogarithmic coordinate system, D_{sL}	0.20 (0.2*)	0.20 (0.5*)
Curve-fitting parameters for the boundary drying curve	—	—
b_i	37	36
c_i	2	0.5
d_i	1.7	1.6
Calculated curve-fitting parameters for the boundary wetting curve	—	—
b_w	4.112	4.151
c_w	2	0.5
d_w	0.85	0.8

Note: *D_{sL} *and* R_{sL} through trial-and-error.

dissolves and breaks apart the bonds between particles, as well as the gypsum crystals present in these soils. As observed before, this unique behavior in gypseous samples has made their behavior different from the regular soil samples. Therefore, this could have led to this different outcome, deviating from the expected results of the mentioned approach.

In an attempt to refine the accuracy of the results, a trial-and-error procedure was employed to adjust the values of D_{sL} and R_{sL}, the parameters that control the distance and slope ratio between the two boundary curves on the SWRC curve are shown in Table 8 and Figure 15. Although the resulting wetting curve exhibited improved compatibility with the experimental results compared to the previous curves, it still fell short of the expected accuracy. It is worth mentioning that since the results of the wetting path using this method did not align well with the experimental results, the curves are reported only for the pure G1 and G2 soil samples.

3.5. Assessment of PTFs for SWRC of Untreated and Cement-Treated Gypsum Soil. Laboratory tests such as pressure plate and suction-controlled oedometer are often time-consuming and costly for obtaining SWRC. An alternative is used to utilize PTFs that establishes the correlations between SWRC and basic soil characteristics. In the current study, the applicability of multiple prevalent PTFs proposed by Zapata et al. [31], Scheinost et al. [33], Saxton et al. [34], and Vereecken et al. [47] was assessed and modified to effectively predict the SWRC of gypseous samples with varying gypsum contents, both untreated and treated with cement. Table 9 summarize

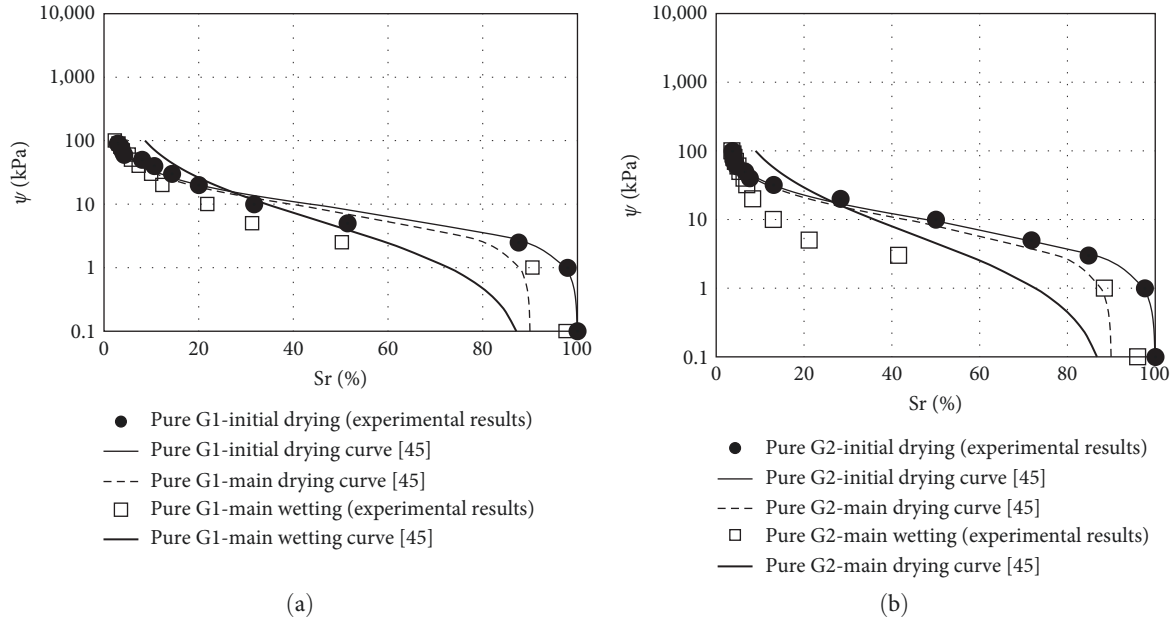

Figure 14: Experimental and fitting curve results for pure (a) G1 and (b) G2.

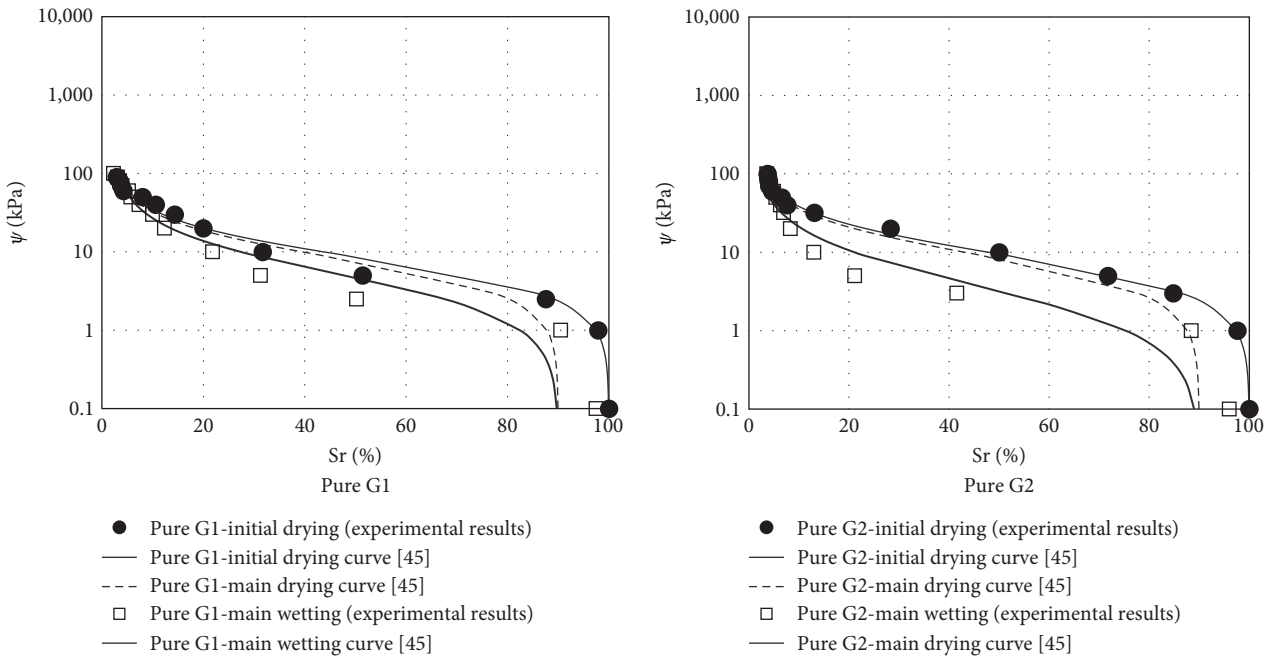

Figure 15: Experimental and fitted wetting curve results for pure G1 and G2 (D_{sL} and R_{sL} through trial-and-error).

these PTFs. These modified PTFs were then compared against results from suction-controlled oedometer tests to assess their prediction accuracy (Figures 16–19).

In particular, Saxton et al. [34] introduced a three-part representation for the SWRC, dividing it into distinct sections: (1) from zero to suction at air entry (AEV); (2) from AEV to 10 kPa; and (3) suctions from 10 to 1,500 kPa and greater. Zapata et al. [31] utilized the Fredlund and Xing [43] equation, correlating fitting parameters with the d60 value obtained from the soil gradation curve. Vereecken et al. [47] employed the fitting equation suggested by Van Genuchten [11] and established correlations between the soil parameters and the fitting parameters (α, n) of that equation. Although the initial Vereecken et al. [47] model did not provide a good match with the experimental results, it was observed that a significant improvement could be achieved through a simple modification.

Table 9: PTFs for predictions of SWRC.

	Range of suction values (kPa)	Equation	
Saxton et al. [34]	From 0.0 to Air-entry value (AEV)	$\theta = \theta_s$	Where: ψ = suction (kPa) AEV = suction at air entry, kPa θ = water content θ_{10} = water content at suction equal to10 kPa θ_s = saturation water content $(\%S)$ = percentage of sand $(\%C)$ = percentage of clay *and* the remaining parameters (a–*v*) are constant coefficients (Saxton et al. [34]; Shahnazari et al. [21])
	From AEV to 10	$\psi = 10.0 - (\theta - \theta_{10}))10.0 - \text{AEV})/(\theta_s - \theta_{10})$ $\theta_{10} = \exp[(2.302 - \ln A)/B]$ $\text{AEV} = 100.0[m + n(\theta_s)]$ $\theta_s = h + j(\%S) + k\log_{10}(\%C)$	
	From 10 to 1,500	$\psi = A\theta^B$ $A = \exp[a + b(\%C) + c(\%S)^2 + b(\%S)^2(\%C)] + 100$ $B = e + f(\%C)^2 + g(\%S)^2 + g(\%S)^2(\%C)$	
Zapata et al. [31] model		$\theta = C\left[\frac{1}{\ln[e+(\frac{\psi}{a})^n]^m}\right]$	Where: $C = 1 - \frac{\ln[1+\frac{\psi}{\psi_r}]}{\ln[1+\frac{10^6}{\psi_r}]}$ $a = 0.8627(d\frac{-0.751}{60})$ $n = 7.5$ $m = 0.7734 + 0.1772\ln(d_{60})$ $\frac{\Psi_r}{a} = \frac{1}{d_{60} + 9.7e^{-4}}$
Vereecken et al. [47] model		$\theta = \theta_r + (\theta_s - \theta_r)[1 + (a\psi)^n]^{-1}$ $\ln(\alpha) = a_0 + a_1\text{Sa} + a_2\text{CL} + a_3\text{C} + a_4\text{BD}$ $\ln(n) = a_5 + a_6\text{Sa} + a_7\text{CL} + a_8\text{Sa}^2$	Sa: sand percentage (%); CL: clay percentage (%); BD: bulk density (kg/m^3) C: carbon content a_0–a_8: constants
Proposed modification of Vereecken et al. [47]		$\theta = \theta_r + (\theta_s - \theta_r)[1 + (a\psi)^n]^{-1}$ $\ln(\alpha) = a_0 + a_1\text{Sa} + a_2\text{CL} + a_3\text{C} + 0.4^* a_4\text{BD}$ $\ln(n) = a_5 + a_6\text{Sa} + a_7\text{CL} + a_8\text{Sa}^2$	

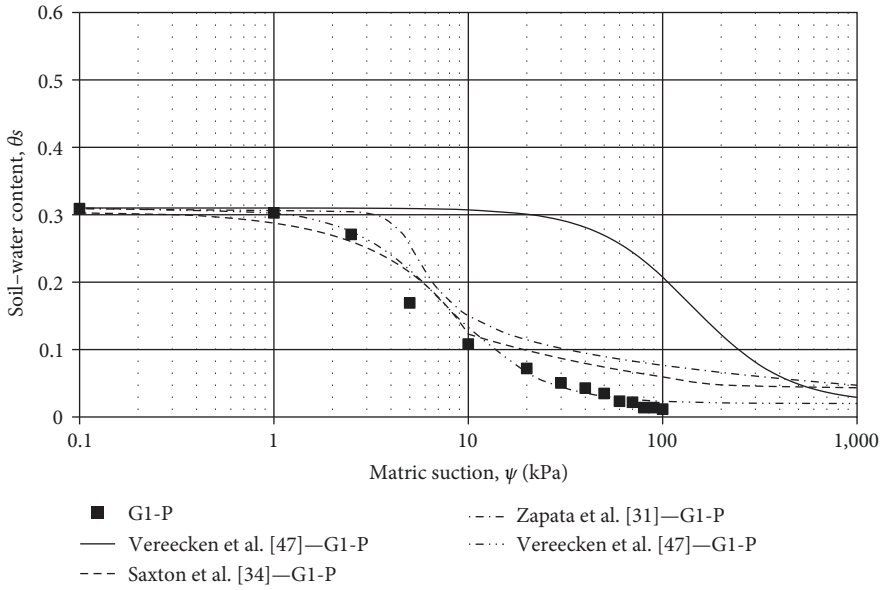

Figure 16: Predicted SWRCs for pure G1-P.

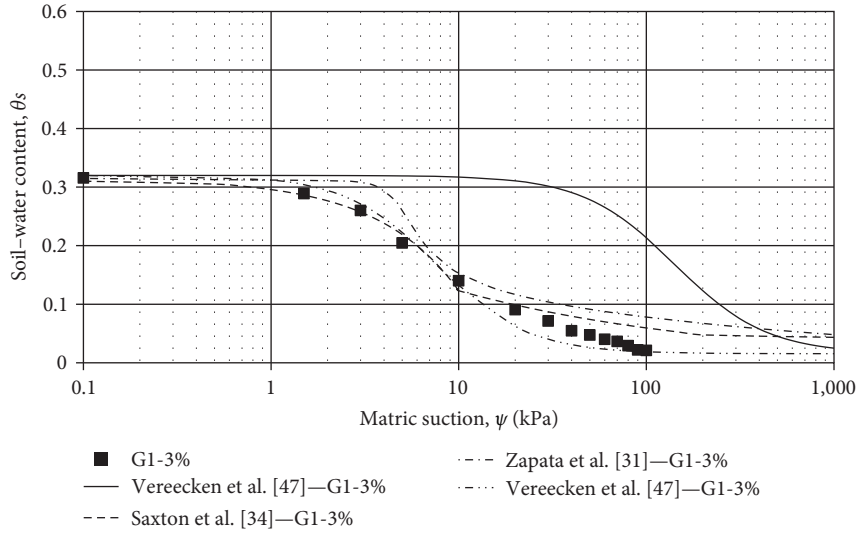

Figure 17: Predicted SWRCs for treated G1-3%.

By incorporating a modification that involved using 0.4 times the bulk density (BD) value in the α formula (e.g., Ln (α) = a0 + a1Sa + a2CL + a3C + 0.4* a4BD), more precise results were obtained for this model. The resulted water retention curve obtained from modified Vereecken model (M-Vereecken 1989) (Figures 16–19) demonstrated accurate predictions of the SWRC of all gypseous soil sample with different gypsum content, treated and untreated.

3.5.1. Assessing the Precision of Employed SWRC Prediction Models. To assess the statistical accuracy of these prediction models, the predicted values from each model were compared to the corresponding test results using the mean-squared error (MSE; Equation 2). Prior studies by Zapata et al. [31] and Shahnazari et al. [21] also employed the MSE as a measure to evaluate various PTFs for predicting SWRC curves:

$$\mathrm{MSE} = \frac{\mathrm{SSE}}{n}, \tag{3}$$

where

MSE = mean-squared error;

SSE = sum of the squared error;

n = number of data points compared.

The MSE values obtained from the three abovementioned PTFs are listed in Table 10. Based on the MSE results, all three models provided reliable predictions for the water retention behavior of gypseous soil with different gypsum content levels, including both treated and untreated samples. Among these models, the modified Vereecken et al. [47] model exhibited the highest level of accuracy, as indicated

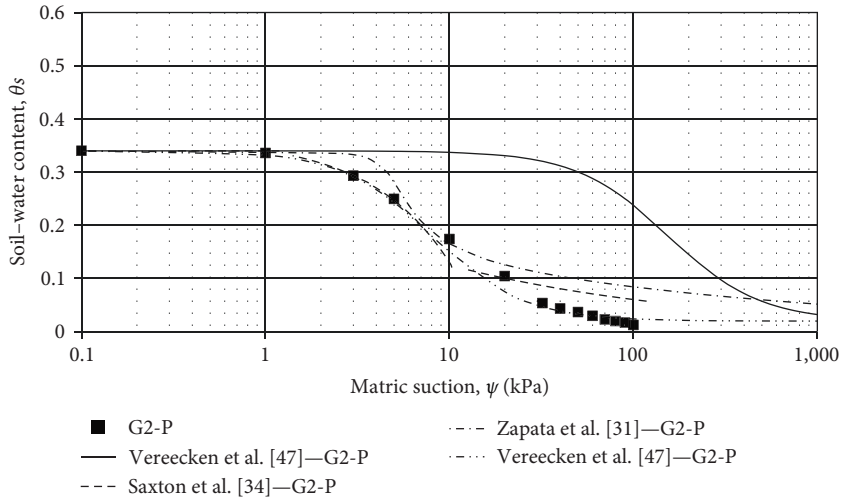

Figure 18: Predicted SWRCs for pure G2-P.

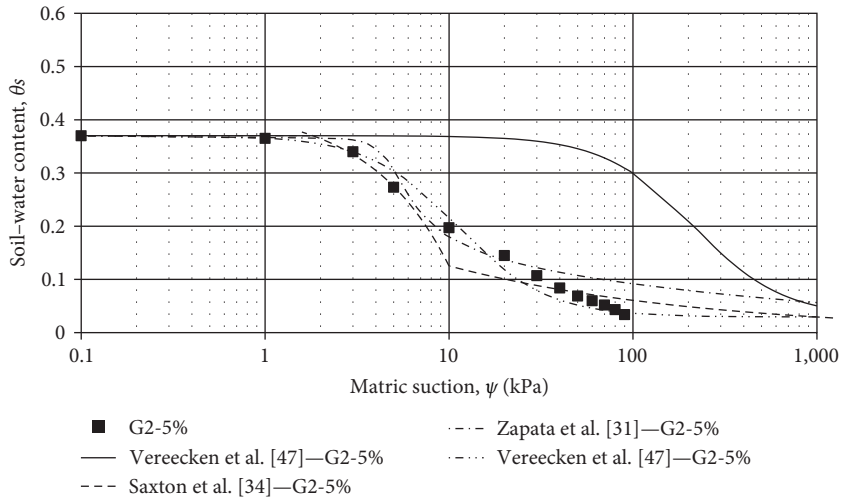

Figure 19: Predicted SWRC for treated G2-5%.

Table 10: MSE values for the evaluated PTFs.

	G1- P	G1- 3%	G2- P	G2- P5%
Saxton et al. [34]	0.001380	0.000594	0.001070	0.000736
Zapata et al. [31]	0.002931	0.00183	0.002665	0.001361
Modified Vereecken et al. [47] model	0.000252	0.00032	0.000129	0.000278

by significantly low-MSE values across all soil samples (e.g., 0.000252, 0.00032, 0.000129, and 0.000278).

To provide a comparison of the MSE values considering previous related studies, it is noteworthy to mention that Zapata et al. [31] conducted evaluations on different soils. Their most accurate PTFs yielded MSE values of 0.000431, 0.002581, and 0.004605 for the three different studied soils. Additionally, Shahnazari et al. [21] investigated calcareous soil samples with three different gradation curves, and the most accurate PTFs resulted in MSE values of 0.002761, 0.000180, and 0.000418, which were obtained using the model proposed by Zapata et al. [31].

4. Conclusions

In this research, the CP of gypseous soils with moderate (G1) and high (G2) gypsum content, as well as their cement-treated samples, was evaluated and compared. The results of SOTs were utilized to assess the CP of untreated and cement-treated samples and determine the optimum

soil–cement mixture for reducing the CP. Additionally, the water retention behavior of treated and untreated gypseous soils was studied using a controlled-suction oedometer, and the effects of cement stabilization on the SWRC in drying and wetting paths were examined. Finally, the performance of widely used PTFs was assessed to discover or modify a reliable method to predict the SWRC of gypsum soil, taking into account both untreated and cement-treated conditions, with satisfactory accuracy. The following results were obtained:

(i) Cement stabilization effectively reduced the CP of both G1 and G2 gypseous soils, as indicated by the SOTs results. With the addition of 3% and 5% cement, the coefficient of collapse decreased by 72% for G1 and 82% for G2, respectively. This shift in CP transformed it from moderate to slight for G1 and from troublesome to slight for G2.

(ii) The controlled-suction oedometer tests demonstrated that cement stabilization significantly influenced the SWRC.

(iii) The SWRC curves of the treated soil, in both the drying and wetting paths, consistently lay above those of the untreated soil, particularly for gypseous soils with high-gypsum content (G2). This can be attributed to the improved bonding and void filling resulting from the soil cementation. As a result, the treated soils exhibited a finer-soil matrix with improved water-retention capacity.

(iv) The impact of cement treatment on the wetting paths was more pronounced compared to the drying paths. This can be due to the changes in the gypseous soil structure caused by water absorption during the wetting path, resulting in more significant differences between the SWRC of treated and untreated samples compared to the drying path.

(v) The differences between the wetting and drying curves of each specimen were more significant in pure gypseous samples compared to the treated soils. This is attributed to the fact that in untreated gypseous samples, the increasing water content during the wetting path gradually dissolves the gypseous bonds between soil particles. However, the cement bindings in treated samples are able to resist the effects of water during the wetting path, leading to less significant changes in the soil–water retention behavior.

(vi) Cement stabilization slightly increased the AEV in both G1 and G2 soils. This is due to the improved pore structure in the treated samples, which increased the pore-size distribution index and subsequently raised the AEV.

(vii) The predictability of commonly used PTFs for the SWRC of gypseous soils was assessed, and it was found that the preexisting PTFs, including those suggested by Saxton et al. [34], Zapata et al. [31], and Vereecken et al. [47], provided acceptable predictions for both treated and untreated gypseous soils. Notably, the modified Vereecken et al. [47] model demonstrated the most accurate predictions for all soil samples in this study.

Data Availability

The experimental data used to support the findings of this study are included within the article.

Conflicts of Interest

The authors declare that they have no conflicts of interest.

References

[1] S. S. Razouki, R. R. Al-Omari, I. H. Nashat, H. F. Razouki, and S. Khalid, "The problems of gypseous soils in Iraq," in *Proceeding of Symposium on the Gypsiferous Soils and Their Effects on Structures*, pp. 7–33, NCCL, Baghdad, 1994.

[2] I. AlNouri and S. Saleam, "Compressibility characteristics of gypseous sandy soils," *Geotechnical Testing Journal*, vol. 17, no. 4, pp. 465–474, 1994.

[3] A. L. Hayal, A. M. B. Al-Gharrawi, and M. Y. Fattah, "Collapse problem treatment of gypseous soil by nanomaterials," *International Journal of Engineering*, vol. 33, no. 9, pp. 1737–1742, 2020.

[4] F. K. Ibrahim, "Improving collapsibility and compressibility of gypseous soil using cement material," *Journal of University of Babylon for Engineering Sciences*, vol. 28, no. 1, pp. 120–131, 2020.

[5] I. H. Obead, M. Y. Fattah, and H. A. Omran, "Role of soluble materials on the hydro-mechanical properties of collapsible gypseous soil," *Transportation Infrastructure Geotechnology*, vol. 10, pp. 1126–1144, 2023.

[6] S. Asghari, M. Ghafoori, and S. S. Tabatabai, "Changes in chemical composition and engineering properties of gypseous soils through leaching: an example from Mashhad, Iran," *Bulletin of Engineering Geology and the Environment*, vol. 77, pp. 165–175, 2018.

[7] A. Johari, H. Golkarfard, F. Davoudi, and A. Fazeli, "A predictive model based on the experimental investigation of collapsible soil treatment using nano-clay in the Sivand Dam region, Iran," *Bulletin of Engineering Geology and the Environment*, vol. 80, pp. 6725–6748, 2021.

[8] A. Johari, H. Golkarfard, F. Davoudi, and A. Fazeli, "Experimental investigation of collapsible soils treatment using nano-silica in the Sivand Dam region, Iran," *Iranian Journal of Science and Technology, Transactions of Civil Engineering*, vol. 46, pp. 1301–1310, 2022.

[9] S. Pongsivasathit, S. Horpibulsuk, and S. Piyaphipat, "Assessment of mechanical properties of cement stabilized soils," *Case Studies in Construction Materials*, vol. 11, Article ID e00301, 2019.

[10] N. Lu and W. J. Likos, *Unsaturated Soil Mechanics*, Wiley, Hoboken, New Jersey, USA, 2004.

[11] M. T. Van Genuchten, "A closed-form equation for predicting the hydraulic conductivity of unsaturated soils," *Soil Science Society of America Journal*, vol. 44, no. 5, pp. 892–898, 1980.

[12] D. G. Fredlund and H. Rahardjo, *Soil Mechanics for Unsaturated Soils*, Wiley, 1993.

[13] E. E. Alonso, A. Gens, and A. Josa, "A constitutive model for partially saturated soils," *Geotechnique*, vol. 40, no. 3, pp. 405–430, 1990.

[14] S. Nazari, M. Hassanlourad, E. Chavoshi, and A. Mirzaii, "Experimental investigation of unsaturated silt–sand soil permeability," *Advances in Civil Engineering*, vol. 2018, Article ID 4946956, 12 pages, 2018.

[15] I. A. Abd, M. Y. Fattah, and H. Mekkiyah, "Relationship between the matric suction and the shear strength in unsaturated soil," *Case Studies in Construction Materials*, vol. 13, Article ID e00441, 2020.

[16] Y.-L. Nan, Z.-K. Zhao, X. Jin, L. Zhang, X.-X. Zhu, and Z.-J. Liu, "Permeability coefficient of unsaturated loess and its gaseous and liquid water migration modeling," *Advances in Civil Engineering*, vol. 2021, Article ID 6689603, 11 pages, 2021.

[17] B. Zamin, H. Nasir, M. A. Sikandar et al., "Comparative study on the field- and lab-based soil–water characteristic curves for expansive soils," *Advances in Civil Engineering*, vol. 2022, Article ID 6390442, 9 pages, 2022.

[18] T. W. Emery, R. I. Stevens, J. Roy, E. Flores, and S. Guthrie, "Characteristic curves for clayey soil treated with cement or lime," in *2020 Intermountain Engineering, Technology and Computing (IETC)*, pp. 1–5, IEEE, Orem, UT, USA, 2020.

[19] S. Kouzegaran, H. Shahnazari, and Y. Jafarian, "The unsaturated shear strength of calcareous soil in comparison with silicate soil," *Marine Georesources & Geotechnology*, vol. 39, no. 2, pp. 200–218, 2021.

[20] G. Tao, D. Lei, L. Liu, Y. Li, and X. Zhu, "Prediction of soil water characteristic curve based on soil water evaporation," *Advances in Civil Engineering*, vol. 2021, Article ID 6686442, 14 pages, 2021.

[21] H. Shahnazari, L. Laloui, S. Kouzegaran, and Y. Jafarian, "Prediction and experimental evaluation of soil–water retention behavior of skeletal calcareous soils," *Bulletin of Engineering Geology and the Environment*, vol. 79, pp. 2395–2410, 2020.

[22] J. Zhang, J. Peng, Y. Chen, J. Li, and F. Li, "Estimation of soil–water characteristic curve for cohesive soils with methylene blue value," *Advances in Civil Engineering*, vol. 2018, Article ID 9213674, 7 pages, 2018.

[23] J. -P. Wang, N. Hu, B. François, and P. Lambert, "Estimating water retention curves and strength properties of unsaturated sandy soils from basic soil gradation parameters," *Water Resources Research*, vol. 53, no. 7, pp. 6069–6088, 2017.

[24] F. Wassar, C. Gandolfi, M. Rienzner, E. A. Chiaradia, and E. Bernardoni, "Predicted and measured soil retention curve parameters in Lombardy region north of Italy," *International Soil and Water Conservation Research*, vol. 4, no. 3, pp. 207–214, 2016.

[25] B. Dolinar, "Prediction of the soil–water characteristic curve based on the specific surface area of fine-grained soils," *Bulletin of Engineering Geology and the Environment*, vol. 74, pp. 697–703, 2015.

[26] C. F. Chiu, W. M. Yan, and K.-V. Yuen, "Estimation of water retention curve of granular soils from particle-size distribution —a Bayesian probabilistic approach," *Canadian Geotechnical Journal*, vol. 49, no. 9, pp. 1024–1035, 2012.

[27] A. Johari, G. Habibagahi, and A. Ghahramani, "Prediction of soil–water characteristic curve using genetic programming," *Journal of Geotechnical and Geoenvironmental Engineering*, vol. 132, no. 5, pp. 661–665, 2006.

[28] A. Johari, G. Habibagahi, and A. Ghahramani, "Prediction of SWCC using artificial intelligent systems: a comparative study," *Scientia Iranica*, vol. 18, no. 5, pp. 1002–1008, 2011.

[29] M. Aubertin, M. Mbonimpa, B. Bussière, and R. P. Chapuis, "A model to predict the water retention curve from basic geotechnical properties," *Canadian Geotechnical Journal*, vol. 40, no. 6, pp. 1104–1122, 2003.

[30] M. D. Fredlund, G. W. Wilson, and D. G. Fredlund, "Use of the grain-size distribution for estimation of the soil–water characteristic curve," *Canadian Geotechnical Journal*, vol. 39, no. 5, pp. 1103–1117, 2002.

[31] C. E. Zapata, W. N. Houston, S. L. Houston, and K. D. Walsh, "Soil–water characteristic curve variability," in *Advances in Unsaturated Geotechnics*, vol. 99, pp. 84–124, Geotechnical Special Publications, 2000.

[32] J. Tomasella and M. G. Hodnett, "Estimating soil water retention characteristics from limited data in Brazilian Amazonia," *Soil Science*, vol. 163, no. 3, pp. 190–202, 1998.

[33] A. C. Scheinost, W. Sinowski, and K. Auerswald, "Regionalization of soil water retention curves in a highly variable soilscape, I. Developing a new pedotransfer function," *Geoder*, vol. 78, no. 3-4, pp. 129–143, 1997.

[34] K. Saxton, W. J. Rawls, J. Romberger, and R. Papendick, "Estimating generalized soil–water characteristics from texture," *Soil Science Society of America Journal*, vol. 50, no. 4, pp. 1031–1036, 1986.

[35] W. J. Rawls and D. L. Brakensiek, "Estimating soil water retention from soil properties," *Journal of the Irrigation and Drainage Division*, vol. 108, no. 2, pp. 166–171, 1982.

[36] L. M. Arya and J. F. Paris, "A physicoempirical model to predict the soil moisture characteristic from particle-size distribution and bulk density data," *Soil Science Society of America Journal*, vol. 45, no. 6, pp. 1023–1030, 1981.

[37] S. C. Gupta and W. E. Larson, "Estimating soil water retention characteristics from particle size distribution, organic matter percent, and bulk density," *Water Resources Research*, vol. 15, no. 6, pp. 1633–1635, 1979.

[38] ASTM D-422, "Standard test methods for particle-size analysis of soils," West Conshohocken, PA, Annual Book of ASTM Standards, ASTM International, 2007.

[39] ASTM D698-00a, "Standard test methods for laboratory compaction characteristics of soil using standard effort (600 kNm/m3)," vol. 4, no. 8, Reprinted from the Annual Book of ASTM Standards. Copyright ASTM, 2012.

[40] ASTM D5333, "Standard test method for measurement of collapse potential of soils," vol. 4, no. 8, Annual Book of ASTM Standards, Copyright, ASTM International, 100 Barr Harbor Drive, P&O Box C700, West Conshohocken, P&A 19428-2959, United States, 2018.

[41] J. E. Jennings and K. Knight, "A guide to construction on or with materials exhibiting additional settlement due to collapse of grain structure," in *Proceeding of 6th Regional Conference for Africa on Soil Mechanics and Foundation Engineering*, pp. 99–105, South Africa, 1975.

[42] L. Laloui, *Mechanics of Unsaturated Geomaterials*, Wiley, New Jersey, 2013.

[43] D. G. Fredlund and A. Xing, "Equations for the soil–water characteristic curve," *Canadian Geotechnical Journal*, vol. 31, no. 4, pp. 521–532, 1994.

[44] M. Feng and D. G. Fredlund, "Hysteretic influence associated with thermal conductivity sensor measurements," in *Proceedings from Theory to the Practice of Unsaturated Soil Mechanics in Association with the 52nd Canadian Geotechnical Conference and the Unsaturated Soil Group*, pp. 14–20, Regina, Sask, 1999.

[45] H. Q. Pham, D. G. Fredlund, and S. L. Barbour, "A study of hysteresis models for soil–water characteristic curves," *Canadian Geotechnical Journal*, vol. 42, no. 6, pp. 1548–1568, 2005.

[46] A. Johari and A. Hooshmand Nejad, "An approach to estimate wetting path of soil–water retention curve from drying path," *Iranian Journal of Science and Technology, Transactions of Civil Engineering*, vol. 42, pp. 85–89, 2018.

[47] H. Vereecken, J. Maes, J. Feyen, and P. Darius, "Estimating the soil moisture retention characteristic from texture, bulk density, and carbon content," *Soil Science*, vol. 148, no. 6, pp. 389–403, 1989.